Journal of Crystal Growth 381 (2013) 6–9

Contents lists available at SciVerse ScienceDirect

Journal of Crystal Growth

journal homepage: www.elsevier.com/locate/jcrysgro

Realization of W–MgZnO epitaxial growth on BeO-buffered ZnO for UV-B photodetectors

H.L. Liang [a,b,c], Z.X. Mei [a,b,c,*], Y.N. Hou [a,b,c], S. Liang [a,b,c], Z.L. Liu [a,b,c], Y.P. Liu [a,b,c], J.Q. Li [a,b,c], X.L. Du [a,b,c,**]

[a] Key Laboratory for Renewable Energy, Institute of Physics, Chinese Academy of Sciences, Beijing 100190, China
[b] Beijing Key Laboratory for New Energy Materials and Devices, Institute of Physics, Chinese Academy of Sciences, Beijing 100190, China
[c] Institute of Physics, Beijing National Laboratory for Condensed Matter Physics, Chinese Academy of Sciences, Beijing 100190, China

ARTICLE INFO

Article history:
Received 29 December 2012
Received in revised form
20 June 2013
Accepted 1 July 2013
Communicated by A. Ohtomo
Available online 8 July 2013

Keywords:
A3. MBE
B3. Photodetector
BeO
UV-B
W–MgZnO

ABSTRACT

A single-phase wurtzite MgZnO film with an optical band gap of 294.5 nm was synthesized on ZnO substrate by molecular beam epitaxy, and a photodetector was fabricated working in the ultraviolet-B spectrum region. Wurtzite BeO was adopted to restrain the substrate response as an insulating layer and provide an excellent epitaxial template for high-Mg-content MgZnO growth. *In situ* reflection high-energy electron diffraction observations, *ex situ* X-ray diffraction and reflectance spectrum indicate the achievement of high-quality single-phase wurtzite MgZnO with smooth surface and deep ultraviolet band gap. The BeO layer efficiently suppresses the photoresponse from the substrate, as the photodetector demonstrates a sharp cutoff at 290 nm, consistent with the optical band gap.

1. Introduction

Wurtzite MgZnO (W–MgZnO) inherits an excellent optoelectronic properties from its parent structure of ZnO, such as tunable wide direct band gap from 3.37 eV to 4.55 eV [1–3], large exciton binding energy (~60 meV) [4], and low growth temperature [5]. These merits make MgZnO a promising candidate as an active layer working in the ultraviolet-B (UV-B, 280–320 nm) spectrum region. UV radiation in this range can be greatly used in many areas such as short-wavelength communication, sterilization and so on. Detection of UV-B rays also has a lot of important applications in conflagration pre-warning, missile detection, and biological sensing, for example. Therefore, great efforts have been devoted to the research on UV-B detection with high-quality, high-Mg-content W–MgZnO components and related issues [6–16].

At present, most W–MgZnO films suitable for deep UV detection were fabricated on Al_2O_3 [10,11] or Si [12,13], where the large lattice mismatch between W–MgZnO and the substrates induced many dislocations in the film, resulting in a deterioration of the device performance. In this case, homo-epitaxial growth of W–MgZnO would be the best choice since commercial ZnO wafers are available. Therefore, a few studies about the fabrication of MgZnO UV-B photodetectors (PDs) on ZnO substrates have been reported [14–16]. A mid-ultraviolet Pt/$Mg_{0.59}Zn_{0.41}O$ Schottky photodiode was fabricated on ZnO wafer, and the photoresponse lower than 10^{-4}A/W was discerned in the wavelength region between 280 and 380 nm, most likely coming from the n^+-ZnO substrate [14]. One effective way to solve this problem may be the insertion of a barrier layer to suppress the carrier transportation from the ZnO side. A conducting polymer named as PEDOT:PSS was used as a Schottky contact and no signal from the substrate was detected [15]. However, considering the unique merits and requirements of MgZnO working in high temperature and high radiation circumstances, unstable organic components must be replaced with stable inorganic materials, like oxides. In this case, insertion of an insulating oxide layer, like MgO, between the MgZnO epilayer and ZnO substrate, may hopefully block the photo-induced carriers in ZnO side and thus solve the above-mentioned problems. However, owing to the large crystal structure difference between wurtzite ZnO and rock-salt MgO, phase

* Corresponding author at: Institute of Physics, Beijing National Laboratory for Condensed Matter Physics, Chinese Academy of Sciences, Beijing 100190, China. Tel.: +86 10 82648062; fax: +86 10 82649542.
** Corresponding author at: Institute of Physics, Beijing National Laboratory for Condensed Matter Physics, Chinese Academy of Sciences, Beijing 100190, China. Tel.: +86 10 82649035; fax: +86 10 82649542
E-mail addresses: zxmei@aphy.iphy.ac.cn, zxmei@iphy.ac.cn (Z.X. Mei), xldu@iphy.ac.cn, xldu@aphy.iphy.ac.cn (X.L. Du).

0022-0248/$ - see front matter © 2013 Elsevier B.V. All rights reserved.
http://dx.doi.org/10.1016/j.jcrysgro.2013.07.001

separation will naturally happen when the film thickness and the Mg solubility reach to the critical values [17], which hinders the increase of Mg content and hence the applications in the UV-B range.

In the present work, an insulating BeO layer is inserted between the active MgZnO layer and the ZnO substrate, serving as an epitaxial template and a barrier layer as well. A high-quality single-phase W–MgZnO with a UV-B band gap was obtained on this BeO interfacial layer with same wurtzite structure. PDs based on this double hetero-structure, *i.e.* W–MgZnO/BeO/ZnO, were fabricated, demonstrating an obvious response in UV-B radiation range, which is in good agreement with the optical band gap determined from the reflectance spectroscopy. More importantly, no signal from the substrate was detected, indicating the role of BeO layer in blocking the carriers from ZnO.

2. Experiment

The single-phase wurtzite MgZnO epitaxial film was fabricated on O-polar ZnO (KMT, $10 \times 10 \times 0.5$ mm^3) substrate by the radio-frequency plasma assisted molecular beam epitaxy (rf-MBE) technique. Elemental Mg, Zn, and Be evaporated by Knudsen cells (CreaTech) and radical oxygen generated by rf-plasma system (SVTA) were used as sources for the growth. The substrate was degreased in acetone and ethanol before loading into the growth chamber. After that, the substrate was thermally cleaned at 750 °C for 20 min and then exposed to oxygen radicals for 20 min at 500 °C to remove the surface defect layer and contaminations caused by the mechanical polishing process. Further, a thin ZnO buffer layer was grown at 500 °C to improve the surface crystalline quality. Subsequently, a single-phase BeO interfacial layer was synthesized at 850 °C with a thickness about 30 nm. At last, MgZnO alloy films were deposited at 450 °C by using a low Mg/Zn flux ratio for the buffer layer and a high Mg/Zn flux ratio for the epilayer. The thickness of the epilayer is around 300 nm.

The whole growth process was *in situ* monitored by reflection high-energy electron diffraction (RHEED), where the evolution of crystal structures and qualities can be clearly seen. The crystal structure of the epilayer was further investigated by *ex situ* X-ray diffraction (XRD) measurements. The band gap of the MgZnO active layer was determined from the reflectance spectroscopy. A UV-B PD was designed and fabricated with a metal–semiconductor–metal (MSM) structure using Ti/Au metal electrodes. Photoresponse measurements were performed using the SpectraPro-500i (Acton Research Corporation) optical system with a Xe-arc lamp combined with a monochromator as the light source.

3. Results and discussion

The RHEED technique was efficiently applied to *in situ* monitor the whole growth process. After the pretreatment of the commercial bulk ZnO substrate with high-temperature thermal cleaning and exposure to oxygen plasma [Fig. 1(a)], a thin ZnO buffer layer was grown to further improve the surface crystalline quality [Fig. 1(b)]. To restrain the strong photoresponse from the substrate, a BeO insulating layer was synthesized [Fig. 1(c)] with a larger space between two reciprocal rods compared to that of ZnO. That is because the in-plane lattice constant of BeO (a=2.699 Å) is smaller than that of ZnO (a=3.249 Å). The spotty patterns herein indicate a 3-dimensional growth and relaxation of lattice strain, which provides a suitable template for the following epitaxial growth of high-quality W–MgZnO, as shown by Fig. 1(d) and (e). In Fig. 1(d), a W–MgZnO buffer layer with low Mg content was subsequently deposited to accommodate the large lattice misfit between BeO and W–MgZnO epilayer with high Mg content. On this quasi-homo buffer layer, a high-quality single-phase W–MgZnO epilayer was achieved with smooth surface, which can be deduced from the sharp streaky patterns in Fig. 1(e). More details about this unique quasi-homo buffer layer growth method can be found in Ref. [3].

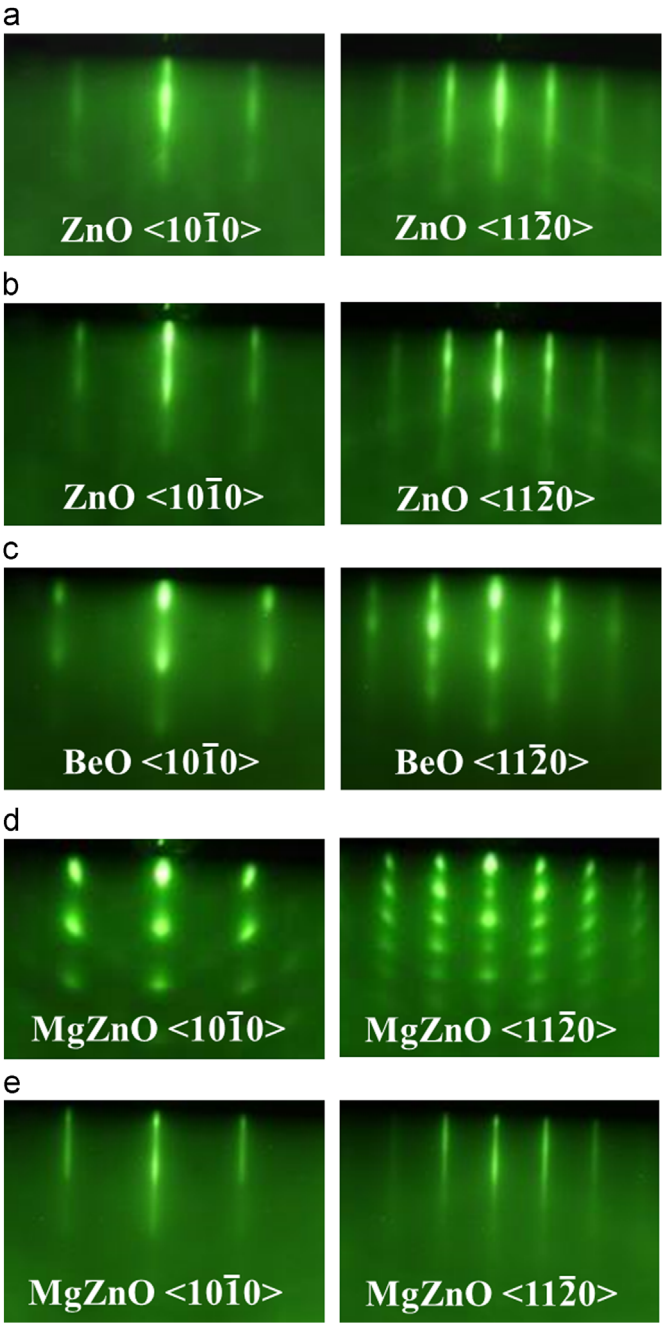

Fig. 1. RHEED patterns along two fixed electron azimuth directions as recorded in sample synthesis: (a) ZnO (0001) substrate after preconditioning, (b) ZnO buffer layer, (c) BeO buffer layer, (d) MgZnO buffer layer after *in-situ* annealing, and (e) MgZnO epilayer after *in-situ* annealing.

To confirm the single wurtzite crystal structure of the epilayer, XRD θ–2θ scan was carried out as demonstrated in Fig. 2. The peak located around 34.44° is attributed to the diffraction from ZnO (002) planes. When Mg is alloyed into the hexagonal lattice of ZnO, the diffraction peak originated from the W–MgZnO (002) planes is shifted to a larger angle (noted as 34.90° in Fig. 2) compared to that from the substrate. It is quite reasonable because

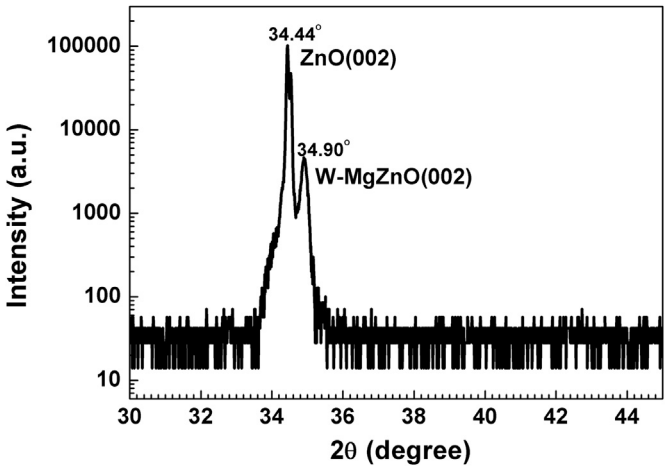

Fig. 2. XRD θ–2θ scan of the MgZnO epilayer. Note: the XRD intensity is rescaled via a logarithmic scale.

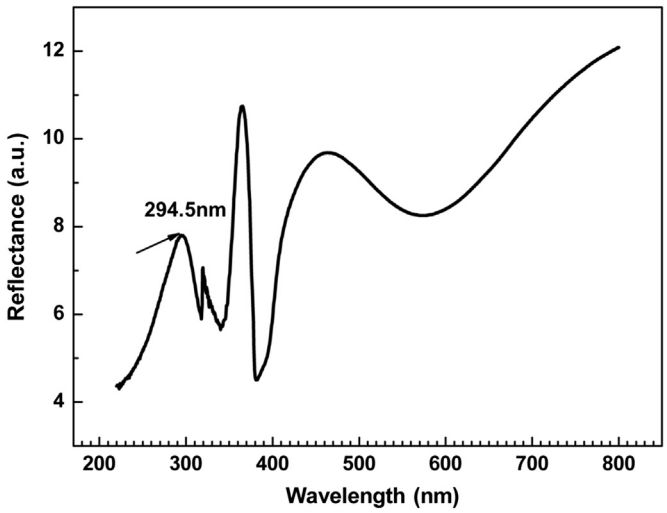

Fig. 3. Reflectance spectrum measured at room temperature. The black arrow indicates the band gap position of the sample.

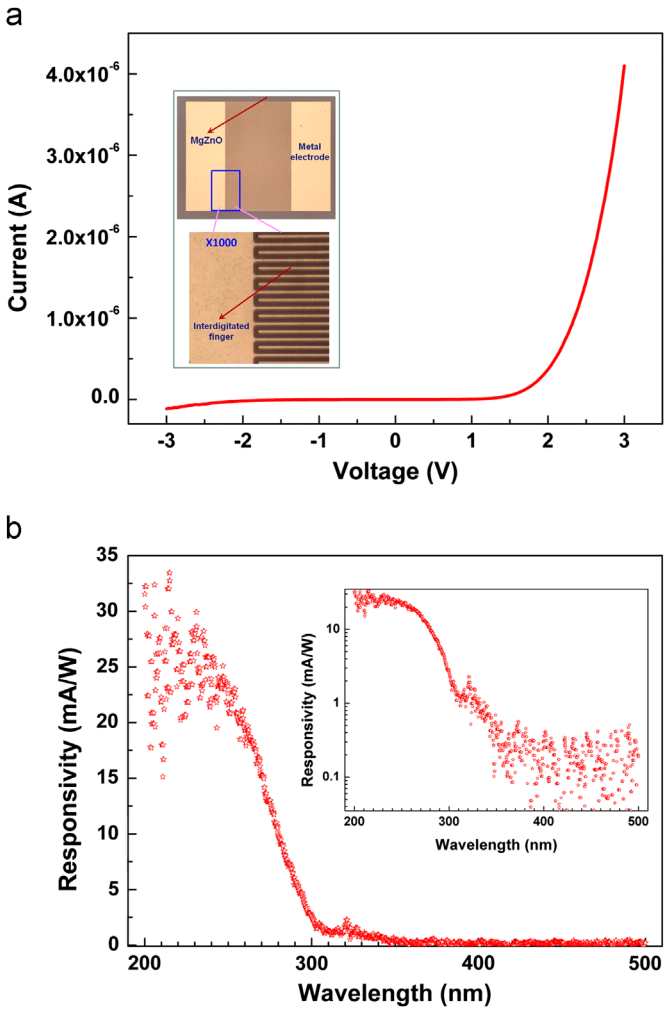

Fig. 4. (a) Current–voltage curve of the W–MgZnO/BeO/ZnO double heterojunction PD and the inset provides the detailed device structure of the PD. (b) Photoresponse spectrum at 0 V bias, and the inset shows the result in a logarithmic scale. Note: the signal located at about 320 nm comes from the shift of the optical gratings.

the plane distance along the growth orientation is decreased due to the smaller ionic radius of Mg^{2+} than that of Zn^{2+} [18]. Moreover, only the two apparently separated peaks related with ZnO (002) and W–MgZnO (002) can be distinguished in the whole scanning scale, indicating a single-crystalline wurtzite structure of the epilayer without the existence of phase separation, which is coincident with the *in situ* RHEED observations.

Room temperature reflectance spectroscopy was applied to determine the band gap of the sample. Fig. 3 shows the measurement result. A characteristic peak [indicated by a black arrow] followed by a typical Fabry–Perot oscillation is exhibited, which can be assigned as the band gap of the epilayer (294.5 nm). In addition, from the relationship between the optical band gap and the Mg content [19], we can estimate that Mg content is about 42%. More importantly, the band gap of the epilayer is within the UV-B range, offering the probable applications of this material as UV-B detecting active layers.

A UV-B PD with a Schottky-type interdigital MSM structure was fabricated. Ti (10 nm)/Au (50 nm) was deposited to form finger electrodes, with 5 μm width, 300 μm length, and 5 μm gap (as shown in the inset of Fig. 4(a)). Current–voltage measurements were carried out, and a non-symmetrical rectifying behavior was observed (seen from Fig. 4(a)), indicating a Schottky contact feature between Ti/Au metal electrode and MgZnO epilayer. Fig. 4(b) shows the photoresponse performance at a bias of 0 V. An obvious cutoff observed at about 290 nm agrees well with the optical band gap determined by the reflectance spectroscopy. The maximum responsivity is ~20 mA/W at 260 nm, and the rejection ratio of UV-B to visible light is about two orders of magnitude, demonstrating that the BeO insulating layer plays a key role in suppressing the strong photoresponse from ZnO substrate at about 370 nm.

4. Conclusions

A single-phase wurtzite MgZnO film with a UV-B band gap was synthesized on O-polar ZnO substrate by using BeO layer to serve as an excellent epitaxial template and to suppress the intensive photoresponse from the substrate. A PD was fabricated on this high-quality active layer with a sharp cutoff wavelength at 290 nm, demonstrating a good response to UV-B radiation. An important contribution of present work is that the signal from ZnO substrate is effectively controlled, opening the potential application of the UV-B optoelectronics based on ZnO substrates.

Acknowledgments

This work was supported by the National Science Foundation (Grant nos. 61076007, 11174348, 51272280, 11274366, and 61204067), the Ministry of Science and Technology of China (Grant nos. 2009 CB929404, 2011CB302002, and 2011CB302006), and the Chinese Academy of Sciences.

References

[1] W. Yang, S.S. Hullavarad, B. Nagaraj, I. Takeuchi, R.P. Sharma, T. Venkatesan, R.D. Vispute, H. Shen, Applied Physics Letters 82 (2003) 3424.
[2] A. Ohtomo, A. Tsukazaki, Semiconductor Science and Technology 20 (2005) S1.
[3] Z.L. Liu, Z.X. Mei, T.C. Zhang, Y.P. Liu, Y. Guo, X.L. Du, A. Hallen, J.J. Zhu, A.Yu. Kuznetsov, Journal of Crystal Growth 311 (2009) 4356.
[4] P. Zu, Z.K. Tang, G.K.L. Wong, M. Kawasaki, A. Ohtomo, H. Koinuma, Y. Segawa, Solid State Communications 103 (1997) 459.
[5] V. Craciun, J. Perriere, N. Bassim, R.K. Singh, D. Craciun, J. Spear, Applied Physics A 69 (1999) S531.
[6] A.K. Sharma, J. Narayan, J.F. Muth, C.W. Teng, C. Jin, A. Kvit, R.M. Kolbas, O.W. Holland, Applied Physics Letters 75 (1999) 3327.
[7] Takako Kenji Yamamoto, Toshiya Tsuboi, Takehiko Ohashi, Hideki Tawara, Atsushi Gotoh, Nakamura, Jiro Temmyo, Journal of Crystal Growth 312 (2010) 1703.
[8] Michael Lorenz, Matthias Brandt, Martin Lange, Gabriele Benndorf, Holger von Wenckstern, Detlef Klimm, Marius Grundmann, Thin Solid Films 518 (2010) 4623.
[9] I. Takeuchi, W. Yang, K.S. Chang, M.A. Aronova, T. Venkatesan, R.D. Vispute, L.A. Bendersky, Journal of Applied Physics 94 (2003) 7366.
[10] Xiaolong Du, Zengxia Mei, Zhanglong Liu, Yang Guo, Tianchong Zhang, Yaonan hou, Ze Zhang, Qikun Xue, Andrej Yu Kuznetsov, Advanced Materials 21 (2009) 4625.
[11] Y.N. Hou, Z.X. Mei, Z.L. Liu, T.C. Zhang, X.L. Du, Applied Physics Letters 98 (2011) 103506.
[12] H.L. Liang, Z.X. Mei, Q.H. Zhang, L. Gu, S. Liang, Y.N. Hou, D.Q. Ye, C.Z. Gu, R.C. Yu, X.L. Du, Applied Physics Letters 98 (2011) 221902.
[13] Y.N. Hou, Z.X. Mei, H.L. Liang, D.Q. Ye, S. Liang, C.Z. Gu, X.L. Du, Applied Physics Letters 98 (2011) 263501.
[14] H. Endo, M. Kikuchi, M. Ashioi, Y. Kashiwaba, K. Hane, Y. Kashiwaba, Applied Physics Express 1 (2008) 051201.
[15] M. Nakano, T. Makino, A. Tsukazaki, K. Ueno, A. Ohtomo, T. Fukumura, H. Yuji, Y. Nishimoto, S. Akasaka, D. Takamizu, K. Nakahara, T. Tanabe, A. Kamisawa, M. Kawasaki, Applied Physics Express 1 (2008) 121201.
[16] Feng Qinghong Zheng, Kai Huang, Jin Ding, Dagui Huang, Zhibing Chen, Zhan, Zhang Lin, Applied Physics Letters 98 (2011) 221112.
[17] Hiroaki Matsui, Hitoshi Tabata, Journal of Applied Physics 99 (2006) 024902.
[18] R.D. Shannon, Acta Crystallographica A 32 (1976) 751.
[19] H. Tampo, H. Shibata, K. Maejima, A. Yamada, K. Matsubara, P. Fons, S. Niki, T. Tainaka, Y. Chiba, H. Kanie, Applied Physics Letters 91 (2007) 261907.